WENTZEL–KRAMERS–BRILLOUIN (WKB) APPROXIMATION

Consider semiclassical motion of a quantum particle in 1 space dimension. Classically, the particle has time-dependent position $x_{\text{cl}}(t)$ and $p_{\text{cl}}(t)$ which obey equations of motion

$$m\frac{dx_{\text{cl}}}{dt} \;=\; p_{\text{cl}}\,, \qquad \frac{dp_{\text{cl}}}{dt} \;=\; -\frac{dV}{dx}@x_{\text{cl}}\,. \tag{1}$$

The best quantum description of this classical motion is a Gaussian wave packet with central position at $x_{\text{cl}}(t)$ and central momentum at $p_{\text{cl}}(t)$. The wave-function of this packet has general form

$$\Psi(x,t) \;=\; C(t) \times \exp\left(\frac{ip_{\text{cl}}(t)\big(x - x_{\text{cl}}(t)\big) - iE_{\text{cl}}t}{\hbar}\right) \times \exp\left(-\frac{\epsilon^2 m^2}{2\hbar^2 p_{\text{cl}}^2(t)} \times \big(x - x_{\text{cl}}(t)\big)^2\right), \tag{2}$$

where the pre-exponential real coefficient $C(t)$ provides for a constant normalization of the wave-packet state,

$$|C(t)|^2 \times \frac{\sqrt{\pi}\hbar|p_{\text{cl}}(t)|}{m\epsilon} \;\equiv\; 1. \tag{3}$$

In the $\epsilon \to 0$ limit, the wave packet (2) spreads out to fill the whole space and takes general form

$$\Psi(x,t) \;=\; \sqrt{\rho(x,t)} \times \exp\left(\frac{i}{\hbar}W(x,t)\right) \tag{4}$$

for some classical function $W(x,t)$; in a moment we shall see that this $W(x,t)$ is the Hamilton's principal function. But for the moment, all we need is $W \gg \hbar$, so the wave-function (4) has a rapidly changing phase $W/\hbar$ while the magnitude $\sqrt{\rho}$ changes much more slowly. So let's plug this wave-function (4) into the time-dependent Schrödinger equation

$$i\hbar\dot{\Psi}(x,t) \;=\; \frac{-\hbar^2}{2m}\Psi''(x,t) \;+\; V(x)\Psi(x,t) \tag{5}$$

where dot denotes a time derivative and a prime denotes an x derivative. The derivatives of the wave-function (4) are

$$i\hbar\dot{\Psi} \;=\; \Psi \times \left(i\hbar\frac{\dot{\rho}}{2\rho} - \dot{W}\right), \tag{6}$$

$$-i\hbar\Psi' = \Psi \times \left(-i\hbar\frac{\rho'}{2\rho} + W'\right), \tag{7}$$

$$-\hbar^2\Psi'' = \Psi \times \left(-i\hbar\frac{\rho'}{2\rho} + W'\right)^2 + \Psi \times \left(-\hbar^2\frac{\rho''\rho - \rho'^2}{2\rho^2} - i\hbar\,W''\right), \tag{8}$$

so plugging them into eq. (5) and dividing both sides by Ψ gives us

$$i\hbar\frac{\dot\rho}{2\rho} - \dot W = \frac{1}{2m}\left(-i\hbar\frac{\rho'}{2\rho} + W'\right)^2 + \frac{1}{2m}\left(-\hbar^2\frac{\rho''\rho - \rho'^2}{2\rho^2} - i\hbar\,W''\right) + V(x). \tag{9}$$

Now let's re-organize the terms in this equation by the powers of $\hbar$:

$$\left(\frac{W'^2}{2m} + \dot W + V(x)\right) - \frac{i\hbar}{2m}\left(W'\frac{\rho'}{\rho} + W'' + m\frac{\dot\rho}{\rho}\right) - \frac{\hbar^2}{2m}\frac{2\rho''\rho - \rho'^2}{4\rho^2} = 0. \tag{10}$$

In particular, the real part of this complex equation is

$$\frac{W'^2}{2m} + \dot W + V(x) = \frac{\hbar^2}{2m} \times \frac{2\rho''\rho - \rho'^2}{4\rho^2} \tag{11}$$

where the LHS is expected to be of classical order of magnitude while the RHS of $O(\hbar^2)$. In the WKB approximation — named after Gregor Wentzel, Hendrik Anthony Kramers, and Léon Brillouin who developed it in 1926 — we neglect the $O(\hbar^2)$ RHS and let

$$\frac{W'^2(x,t)}{2m} + \dot W(x,t) + V(x) = 0. \tag{12}$$

In classical mechanics, eq. (12) is the *Hamilton–Jacobi equation for the Hamilton's principle function $W(x,t)$ for the 1d particle.*

Aside: In classical mechanics of n dynamical variables $q_1(t), \ldots, q_n(t)$ — collectively described by $Q(t)$ — the Hamilton's principal function $W(Q;t)$ is defined as follows. Pick a fixed starting point Q^0 at a fixed stating time t^0, and find a classical trajectory $Q(t)$ leading from Q^0 at time t^0 to some desired Q^f at time t^f; then $W(Q^f, t^f)$ is the classical action of this trajectory,

$$W(Q^f; t^f) = \int_{t^0}^{t^f} L(Q, \dot Q, t)\, dt. \tag{13}$$

As a function of the end point (Q^f, t^f) for a fixed starting point (Q^0, t^0), this action obeys the Hamilton–Jacobi equation

$$\frac{\partial}{\partial t^f}W(Q^f; t) + H(Q^f; P^f; t^f) = 0 \quad \text{for} \quad p_i^f = \frac{\partial W}{\partial q_i^f}. \tag{14}$$

In particular, for a 1d particle with classical Hamiltonian $H(x,p) = V(x) + p^2/2m$, the Hamilton–Jacobi equation becomes (12).

Coming back to quantum mechanics and the WKB approximation, for a stationary state

$$\Psi(x,t) \;=\; \Psi(x) \times e^{-iEt/\hbar} \quad \Longrightarrow \quad W(x,t) \;=\; W(x) \;-\; Et \tag{15}$$

while $W(x)$ obeys

$$\frac{1}{2m} W'^2 \;-\; E \;+\; V(x) \;=\; 0. \tag{16}$$

In other words,

$$\frac{dW}{dx} \;=\; p_{\mathrm{cl}}(x) \;=\; \pm\sqrt{2m(E - V(x))} \tag{17}$$

is the classical momentum of the particle of net energy E at the moment it happens to be at the point x with potential $V(x)$. Consequently,

$$W(x) \;=\; \mathrm{const} \;\pm\; \int dx\,\sqrt{2m(E - V(x))}\,. \tag{18}$$

Eq. (18) determines the phase of the wave function in the WKB approximation. As to the magnitude $\sqrt{\rho}$, it follows from the imaginary part of eq. (10):

$$\frac{i\hbar}{2m}\left(W'\frac{\rho'}{\rho} + W'' + m\frac{\dot{\rho}}{\rho}\right) \;=\; 0, \tag{19}$$

hence

$$m\dot{\rho} \;=\; -\,W'\rho' \;-\; W''\rho \;=\; -(W'\rho)'. \tag{20}$$

Physically, we may interpret this equation as the *continuity* equation of a particle beam with density $\rho(x,t) = |\Psi(x,t)|^2$ and velocity $v(x,t) = W'(x,t)/m$ — cf. eq. (17), — hence flux density $\mathcal{F} = \rho v = \rho W'/m$, thus

$$\dot{\rho} \;+\; \mathcal{F}' \;=\; 0 \quad \Longrightarrow \quad \dot{\rho} \;=\; -\frac{1}{m}(W'\rho)'. \tag{21}$$

For a stationary state $\dot{\rho} = 0$, so eq. (20) becomes $(W'\rho)' = 0$ and hence

$$\rho(x) \;=\; \frac{\mathrm{const}}{W'(x)} \;=\; \frac{\mathrm{const}}{|p_{\mathrm{cl}}(x)|} \;=\; \frac{\mathrm{const}}{\sqrt{2mE - V(x)}}\,. \tag{22}$$

3

To simplify future formulae, let

$$k(x) \;=\; \frac{|p_{\mathrm{cl}}(x)|}{\hbar} \;=\; +\frac{\sqrt{2m(E - V(x))}}{\hbar}\,; \tag{23}$$

then in the WKB approximation

$$W'(x) \;=\; \pm\hbar k(x) \quad\Longrightarrow\quad \frac{W(x)}{\hbar} \;=\; \text{const} \;\pm\; \int k(x)\,dx \tag{24}$$

while

$$\rho(x) \;=\; \frac{\text{const}}{k(x)}\,, \tag{25}$$

thus

$$\Psi_{\mathrm{WKB}}(x) \;=\; \frac{\text{const}}{\sqrt{k(x)}} \times \exp\left(\pm i \int^x k(x')\,dx' \right). \tag{26}$$

Or if we allow motion in both directions,

$$\Psi_{\mathrm{WKB}}(x) \;=\; \frac{A}{\sqrt{k(x)}} \times \exp\left(+i \int^x k(x')\,dx' \right) \;+\; \frac{B}{\sqrt{k(x)}} \times \exp\left(-i \int^x k(x')\,dx' \right) \tag{27}$$

for some constants A and B.

Before we illustrate the WKB wave-functions (27) with specific examples, consider the limits of applicability of the WKB approximation.

1. As written, eq. (27) applies only in the classically allowed ranges of x where $V(x) < E$. However, it may be analytically continued to the classically forbidden regions, as we shall see in a moment.

2. The WKB approximation presumes that the phase $W(x)/\hbar$ changes with x much more rapidly then the magnitude $\rho(x)$ — that's how we are able to neglect the $O(\hbar^2)$ terms

in eq. (10). Thus, we need

$$k(x) \ \gg \ \frac{|\rho'(x)|}{\rho(x)} \ = \ \frac{|k'(x)|}{k(x)}, \tag{28}$$

or in terms of the potential $V(x)$,

$$\frac{\sqrt{2m(E - V(x))}}{\hbar} \ \gg \ \frac{|V'(x)|}{E - V(x)} \quad \Longrightarrow \quad \sqrt{2m}\big(E - V(x)\big)^{3/2} \ \gg \ \hbar|V'(x)| \ = \ \hbar|F(x)| \tag{29}$$

where $F(x) = -V'(x)$ is the force acting on the particle. Any discontinuity of the potential $V(x)$ — such as at the ends of a square well or a square barrier — leads to enormous forces $F(x) \sim \delta(x - x_{\mathrm{disc}})$ which break the limit (29). Thus, the WKB approximation works only for continuous potentials.

On the other hand, for a continuous potential $V(x)$, the inequality (29) holds *almost* everywhere in the classically allowed region, except very close to the classical turning points x_t where $V(x_t) = E$. At microscopically short $O(\hbar^{2/3})$ distances from the classical turning points the inequality (29) fails, and the WKB approximation becomes invalid. Specifically, let $F(x_t)$ be the force acting on a particle at a turning point x_t. Then, microscopically close to this turning point,

$$F(x) \ \approx \ F(x_t), \quad E \ - \ V(x) \ \approx \ F(x_t) \times (x - x_t), \tag{30}$$

so the limit (29) becomes

$$\sqrt{2m}|F(x_t)|^{3/2}|x - x_t|^{3/2} \ \gg \ \hbar|F(x_t)| \quad \Longrightarrow \quad |x - x_t| \ \gg \ \frac{\hbar^{2/3}}{\sqrt[3]{2m|F(x_t)|}}. \tag{31}$$

- The bottom line is, the WKB approximation (27) is valid for a continuous potential $V(x)$ in the classically allowed region $V(x) < E$, but not too close to the classical turning points, *cf.* eq. (31).

Forbidden Regions

The WKB wave-function allowed can be analytically continued from the classically allowed to the classically forbidden regions of space. In the forbidden regions of $V(x) > E$,

$$k = \frac{\sqrt{2m(E - V(x))}}{\hbar} \tag{32}$$

becomes imaginary,

$$k = i\kappa \quad \text{for} \quad \kappa = +\frac{\sqrt{2m(V(x) - E)}}{\hbar}, \tag{33}$$

so the WKB wave-function becomes

$$\Psi_{\text{WKB}}(x) = \frac{C}{\sqrt{\kappa(x)}} \times \exp\left(-\int^x \kappa(x')\, dx'\right) + \frac{D}{\sqrt{\kappa(x)}} \times \exp\left(+\int^x \kappa(x')\, dx'\right) \tag{34}$$

for some constants C and D.

Unlike the WKB approximation for the classically allowed region, in the classically forbidden region we cannot justify the wave-functions (34) via semiclassical analysis of wave-packets. Instead, we may simply check that the forbidden-region WKB wave-functions (34) obey the time-independent Schrödinger equation up to terms of relative order $O(\hbar^2)$. For simplicity, let's focus on a single exponential

$$\Psi_{\text{WKB}}(x) = \frac{\text{const}}{\sqrt{\kappa(x)}} \times \exp\left(\pm \int^x \kappa(x')\, dx'\right), \tag{35}$$

hence

$$\Psi'_{\text{WKB}}(x) = \Psi_{\text{WKB}}(x) \times \left(-\frac{\kappa'(x)}{2\kappa(x)} \pm \kappa(x)\right), \tag{36}$$

$$\Psi''_{\text{WKB}}(x) = \Psi_{\text{WKB}}(x) \times \left(-\frac{\kappa'(x)}{2\kappa(x)} \pm \kappa(x)\right)^2 + \Psi_{\text{WKB}}(x) \times \left(-\frac{\kappa'(x)}{2\kappa(x)} \pm \kappa(x)\right)' \tag{37}$$

and therefore

$$
\begin{aligned}
\frac{\Psi''_{\mathrm{WKB}}}{\Psi_{\mathrm{WKB}}} &= \left(-\frac{\kappa'}{2\kappa} \pm \kappa \right)^2 + \left(-\frac{\kappa'}{2\kappa} \pm \kappa \right)' \\
&= \kappa^2 \mp \kappa' + \frac{\kappa'^2}{4\kappa^2} \pm \kappa' - \frac{\kappa''\kappa - \kappa'^2}{2\kappa^2} \\
&= \kappa^2 + \left(\frac{3\kappa'^2 - 2\kappa''\kappa}{4\kappa^2} = \sqrt{\kappa}\left(\frac{1}{\sqrt{\kappa}}\right)'' \right) \\
&= \frac{2m(V - E)}{\hbar^2} + \sqrt[4]{V - E}\left(\frac{1}{\sqrt[4]{V - E}}\right)''
\end{aligned}
\tag{38}
$$

where the first term on the bottom line is $O(1/\hbar^2)$ because of the implicit depencence of Ψ_{WKB} on the $\hbar$ while the second term is $O(1)$. In the context of the Schrödinger equation,

$$
\frac{-\hbar^2}{2m}\frac{\Psi''_{\mathrm{WKB}}(x)}{\Psi_{\mathrm{WKB}}(x)} + V(x) - E = \frac{-\hbar^2}{2m} \times \sqrt[4]{V - E}\left(\frac{1}{\sqrt[4]{V - E}}\right)'' = O(\hbar^2) \approx 0, \quad (39)
$$

which makes the wave-functions $\Psi_{\mathrm{WKB}}(x, t)$ approximately obey the Schrödinger equation. The approximation here is similar to what we have used in the WKB approximation for the classically allowed regions, and that's why we call these wave-functions (34) *the WKB-approximate wave-functions for the classically forbidden region(s).*

Similarly to the classically allowed case, the WKB approximation for the classically forbidden regions breaks down when the pre-exponential factor $1/\sqrt{\kappa}$ changes faster than the exponent. For a continuous potential $V(x)$ this happens only in the microscopic vicinity of a classical turning point x_t where $V(x_t) = E$. The detailed analysis closely parallels the classically-allowed case, so let me simply state the result: The WKB approximate wave-functions (34) work for $V(x) > E$ and not too close to the turning points, specifically

$$
|x - x_t| \gg \frac{\hbar^{2/3}}{\sqrt[3]{2m|F(x_t)|}}
\tag{31}
$$

where $F(x) = -V'(x)$ is the potential force on the particle.

Boundary Layers

Consider the neighborhood of a classical turning point x_t:

$$\text{(40)}$$
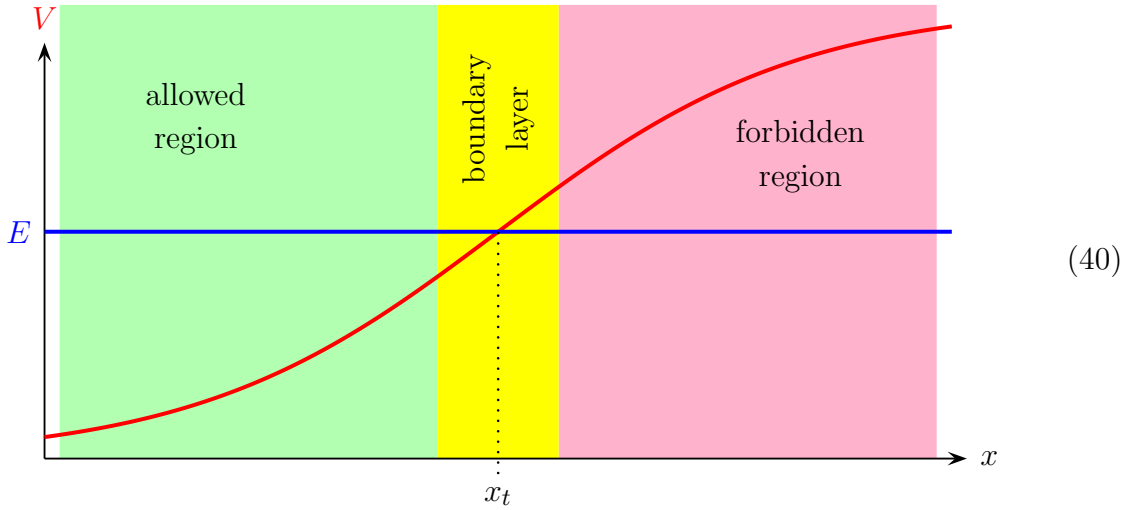
We have WKB approximations for the wave-functions in both classically allowed and classically forbidden regions, but both of these approximations break down in the narrow boundary layer around the classical turning point x_t. To solve for the wave-function in the boundary layer, we need a different approximation based on the narrow $O(\hbar^{2/3})$ width of this layer, *cf.* eq. (31). For a classical-scale potential $V(x)$, we may treat the force $F(x) = -V'(x)$ as approximately constant withing the boundary layer, hence approximately linear potential

$$V(x) \approx V(x_t) - F(x_t) \times (x - x_t) = E - F(x_t) \times (x - x_t). \tag{41}$$

For this potential, the Schrödinger equation becomes

$$-\frac{\hbar^2}{2m} \frac{d^2\Psi}{dx^2} = F(x_t) \times (x - x_t) \times \Psi(x), \tag{42}$$

which becomes the Airy equation

$$\frac{d^2\Psi}{dz^2} = z \times \Psi(z) \tag{43}$$

after a linear change of variable

$$z = -\operatorname{sign}(F(x_t)) \times \sqrt[3]{\frac{2m|F(x_t)|}{\hbar^2}} \times (x - x_t) \tag{44}$$

In terms of z:

— the allowed region lies at large negative z;

— the forbidden region lies at large positive z;

— the boundary layer spans small and moderate z of either sign.

The Airy equations and its 2 independent solutions — called the *regular Airy function* $Ai(z)$ and the *irregular Airy function* $Bi(z)$ — are explained in detail in my notes on Airy functions. For the moment, let me simply plot the two functions:
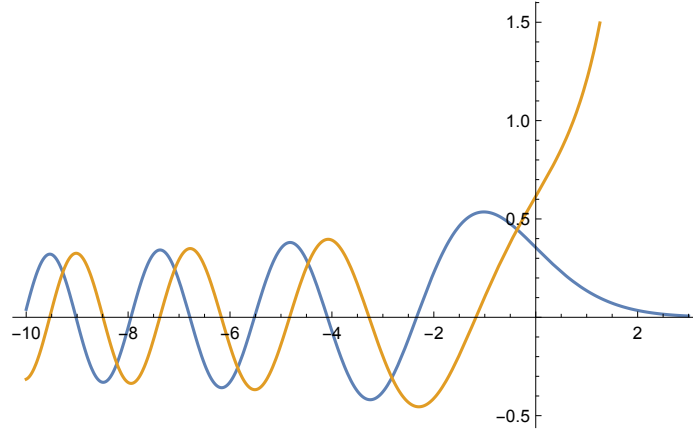
For positive z, the regular Airy function Ai (blue) rapidly decreases to zero while the irregular Airy function Bi (red) blow up to $+\infty$. On the other hand, for negative z, both Airy functions oscillate with a slowly decreasing amplitude as $z \to 0$. Asymptotically, for $z \to +\infty$

$$Ai(z) \;\approx\; \frac{1}{2\sqrt{\pi}\,z^{1/4}} \times \exp\left(-\tfrac{2}{3}z^{3/2}\right), \tag{45}$$

$$Bi(z) \;\approx\; \frac{1}{\sqrt{\pi}\,z^{1/4}} \times \exp\left(+\tfrac{2}{3}z^{3/2}\right), \tag{46}$$

while for $z \to -\infty$

$$Ai(z) \;\approx\; \frac{1}{\sqrt{\pi}\,|z|^{1/4}} \times \sin\left(\tfrac{\pi}{4} + \tfrac{2}{3}|z|^{3/2}\right), \tag{47}$$

$$Bi(z) \;\approx\; \frac{1}{\sqrt{\pi}\,|z|^{1/4}} \times \cos\left(\tfrac{\pi}{4} + \tfrac{2}{3}|z|^{3/2}\right). \tag{48}$$

All of these asymptotics are in perfect agreement with the WKB approximate wave functions on the forbidden and allowed sides of a turning point for a linear potential $V =$

$E - F(x - x_t)$. Indeed, let $F < 0$ as on the diagram (40); then on the forbidden side $x > x_t$, $z > 0$ we have

$$\kappa(x) = \frac{\sqrt{2m|F|(x - x_t)}}{\hbar} \quad \Longrightarrow \quad \int_{x_t}^{x} \kappa(x')\,dx' = \frac{2}{3}\frac{\sqrt{2m|F|}}{\hbar} \times (x - x_t)^{3/2} = \frac{2}{3}z^{3/2}, \quad (49)$$

hence

$$\Psi_{\text{WKB}}(z) \; \propto \; \frac{1}{z^{1/4}} \times \exp\bigl(\pm\tfrac{2}{3}z^{3/2}\bigr), \tag{50}$$

in perfect agreement with eqs. (45) and (46) for the Airy functions of $z \to +\infty$. Likewise, on the allowed side $x < x_t$, $z < 0$ of the turning point,

$$k(x) = \frac{\sqrt{2m|F|(x_t - x)}}{\hbar} \quad \Longrightarrow \quad \int_{x}^{x_t} k(x')\,dx' = \frac{2}{3}\frac{\sqrt{2m|F|}}{\hbar} \times (z_t - x)^{3/2} = \frac{2}{3}|z|^{3/2}, \quad (51)$$

hence

$$\Psi_{\text{WKB}}(z) \; \propto \; \frac{1}{|z|^{1/4}} \times \exp\bigl(\pm i \times \tfrac{2}{3}|z|^{3/2}\bigr), \tag{52}$$

thus two linear combinations of these WKB solutions

$$\frac{1}{|z|^{1/4}} \times \sin\bigl(\tfrac{\pi}{4} + |z|^{3/2}\bigr) \quad \text{and} \quad \frac{1}{|z|^{1/4}} \times \cos\bigl(\tfrac{\pi}{4} + |z|^{3/2}\bigr) \tag{53}$$

are in perfect agreement with eqs. (47) and (48) for the Airy functions of $z \to -\infty$.

Now consider the Schrödinger equation for a more general potential, so the linear potential approximation $V(x) - E \approx -F(x - x_t)$ is valid only within the thin boundary later around the turning point x_t. However, let's assume that this boundary layer is thick enough to include large positive $z \gg 1$ on the forbidden side of the layer and large negative z on the allowed side. In this setup, the Airy-function solutions within the boundary layer tell us how to connect a specific combination of the two WKB wave-functions on the allowed side of the turning point with a specific combinations of the two WKB wave functions on the

forbidden side. Indeed, take the regular Airy function solution for the boundary layer,

$$\Psi_1(z) = C_1 \left(\frac{\pi^3 \hbar^2}{2M|F|} \right)^{1/6} \times Ai(z) \tag{54}$$

for some overall coefficient C_1. Then for large positive z (but for x within the boundary layer)

$$\Psi_1(x) \approx C_1 \left(\frac{\hbar^2}{2M|F|} \right)^{1/6} \times \frac{1}{2z^{1/4}} \exp\left(-\tfrac{2}{3}z^{3/2}\right) = \frac{C_1}{2\sqrt{\kappa(x)}} \exp\left(-\int_{x_t}^{x} \kappa(x')dx' \right), \tag{55}$$

which then analytically continues to x in the forbidden zone beyond the boundary layer as the specific WKB solution

$$\Psi_1(x) \approx \frac{C_1}{2\sqrt{\kappa(x)}} \exp\left(-\int_{x_t}^{x} \kappa(x')dx' \right). \tag{56}$$

At the same time, for large negative z (but x within the boundary later), the same regular Airy function solution becomes

$$\Psi_1(x) \approx C_1 \left(\frac{\hbar^2}{2M|F|} \right)^{1/6} \times \frac{1}{|z|^{1/4}} \sin\left(\tfrac{\pi}{4} + \tfrac{2}{3}|z|^{3/2}\right) = \frac{C_1}{\sqrt{k(x)}} \exp\left(\frac{\pi}{4} + \int_{x}^{x_t} k(x')dx' \right), \tag{57}$$

which then analytically continues to x in the allowed zone beyond the boundary layer as the specific WKB solution

$$\Psi_1(x) \approx \frac{C_1}{\sqrt{k(x)}} \sin\left(\frac{\pi}{4} + \int_{x}^{x_t} k(x')dx' \right). \tag{58}$$

Note the same coefficient C_1 in eqs. (56) and (58).

Likewise, take the irregular Airy function solution for the boundary layer

$$\Psi_2(z) \;=\; C_2 \left(\frac{\pi^3 \hbar^2}{2M|F|} \right)^{1/6} \times Bi(z) \tag{59}$$

for some other overall coefficient C_2. For a large positive z (but x within the boundary layer), this solution becomes

$$\Psi_2(x) \;\approx\; C_2 \left(\frac{\hbar^2}{2M|F|} \right)^{1/6} \times \frac{1}{z^{1/4}} \exp\!\left(+\tfrac{2}{3} z^{3/2}\right) \;=\; \frac{C_2}{\sqrt{\kappa(x)}} \exp\left(+ \int_{x_t}^{x} \kappa(x')dx' \right), \tag{60}$$

which then analytically continues to x in the forbidden zone beyond the boundary layer as a different WKB solution from (56), namely

$$\Psi_2(x) \;\approx\; \frac{C_1}{\sqrt{\kappa(x)}} \exp\left(+ \int_{x_t}^{x} \kappa(x')dx' \right). \tag{61}$$

At the same time, for large negative z (but x within the boundary later), the same irregular Airy function solution becomes

$$\Psi_2(x) \;\approx\; C_2 \left(\frac{\hbar^2}{2M|F|} \right)^{1/6} \times \frac{1}{|z|^{1/4}} \cos\!\left(\tfrac{\pi}{4} + \tfrac{2}{3}|z|^{3/2}\right) \;=\; \frac{C_2}{\sqrt{k(x)}} \cos\left(\frac{\pi}{4} + \int_{x}^{x_t} k(x')dx' \right), \tag{62}$$

which then analytically continues to x in the allowed zone beyond the boundary layer as the WKB solution

$$\Psi_2(x) \;\approx\; \frac{C_2}{\sqrt{k(x)}} \cos\left(\frac{\pi}{4} + \int_{x}^{x_t} k(x')dx' \right). \tag{63}$$

Again, we have the same coefficient C_2 in eqs. (61) and (63).

Altogether, between eqs. (56), (58), (61), and (63), we see which WKB solution on the classically forbidden side come with which WKB solutions on the classically allowed side and

12

vice verse:

on the forbidden side $x > x_t$

$$\Psi_{\mathrm{WKB}}(x) = \frac{C_1}{2\sqrt{\kappa(x)}} \exp\left(-\int_{x_t}^{x} \kappa(x')dx'\right) + \frac{C_2}{\sqrt{\kappa(x)}} \exp\left(+\int_{x_t}^{x} \kappa(x')dx'\right),$$

on the allowed side $x < x_t$

$$\Psi_{\mathrm{WKB}}(x) = \frac{C_1}{\sqrt{k(x)}} \sin\left(\frac{\pi}{4} + \int_{x}^{x_t} k(x')dx'\right) + \frac{C_2}{\sqrt{k(x)}} \cos\left(\frac{\pi}{4} + \int_{x}^{x_t} k(x')dx'\right),$$

(64)

for the same WKB solution $\Psi_{\mathrm{WKB}}(x)$.

Note that although we have derived eq. (64) from the Airy functions and their asymptotic behavior at $z \to \pm\infty$, *we do not need the airy functions to use this formula!* Instead, we may use some Physics considerations to choose a specific WKB solution on one side of the turning point, and then eq. (64) will pick the right WKB solution on the other side. We shall specific examples of such choices in the following sections of these notes in the context of bound states of potential wells and quantum tunneling through potential barriers.

Potential Wells

Next, consider a bound state of a particle in a potential well. Classically, there is an allowed region inside the well bounded by two turning points x_1 and x_2, and the particle bounces back and forth between these turning points; the regions to the left of the x_1 or to the right of the x_2 are classically forbidden. In quantum mechanics, we have the following situation:

(65)
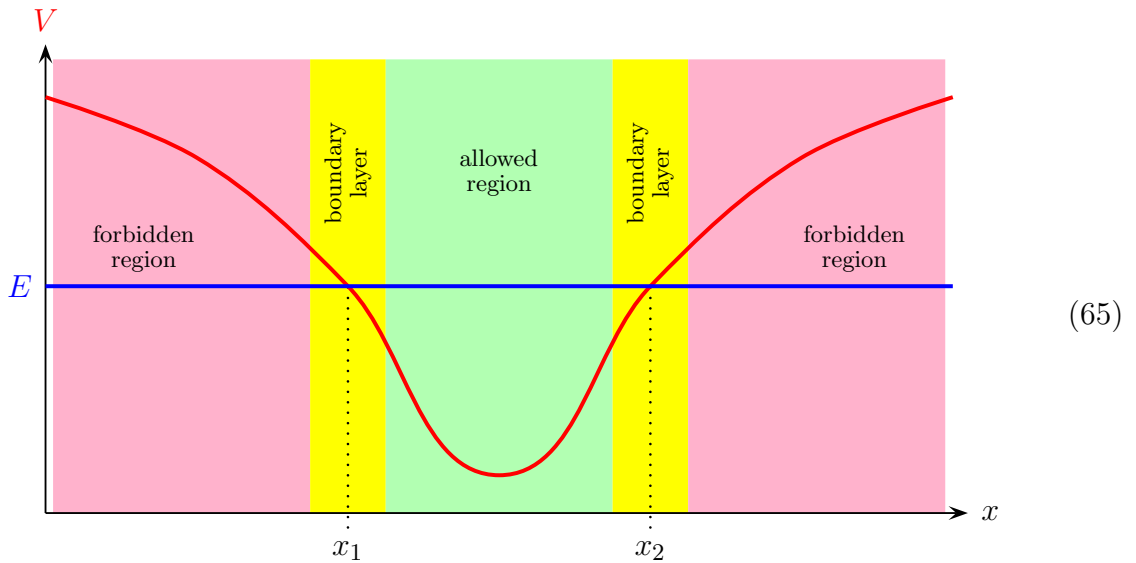
Let's assume that the well is deep and wide enough to use the WKB approximation, and that the two forbidden regions extend all the way to infinity. Consequently, the wave-function in the left forbidden region must die out for $x \to -\infty$ and in the right forbidden region for $x \to +\infty$. Consequently, in the WKB approximation

$$
\begin{aligned}
&\text{for } x < x_1 - O(\hbar^{2/3}): \\
&\qquad \Psi(x) = \frac{C_1}{\sqrt{\kappa(x)}} \times \exp\left(-\int_x^{x_1} \kappa(x')\, dx' \right), \\
&\text{for } x > x_2 + O(\hbar^{2/3}): \\
&\qquad \Psi(x) = \frac{C_2}{\sqrt{\kappa(x)}} \times \exp\left(-\int_{x_2}^{x} \kappa(x')\, dx' \right),
\end{aligned}
\tag{66}
$$

$\langle\!\langle$ note limits of the two integrals! $\rangle\!\rangle$

for some coefficients C_1 and C_2. At the same time, for the allowed region inside the well, the WKB approximation gives us

$$
\begin{aligned}
\Psi(x) &= \frac{A_1}{\sqrt{k(x)}} \times \exp\left(+i\int_{x_1}^{x} k(x')dx' \right) + \frac{B_1}{\sqrt{k(x)}} \times \exp\left(-i\int_{x_1}^{x} k(x')dx' \right) \\
&= \frac{A_2}{\sqrt{k(x)}} \times \exp\left(-i\int_{x}^{x_2} k(x')dx' \right) + \frac{B_2}{\sqrt{k(x)}} \times \exp\left(+i\int_{x}^{x_2} k(x')dx' \right)
\end{aligned}
\tag{67}
$$

for some coefficients A_1 and B_1, or equivalently A_2 and B_2. To relate all these coefficients to each other, we use the Airy function matching conditions (64) at the turning points x_1 and x_2. Specifically, for the wave functions (66) in the forbidden regions, the matching condition at x_1 tells us that in the allowed region we must have

$$
\Psi(x) = \frac{2C_1}{\sqrt{k(x)}} \times \sin\left(\frac{\pi}{4} + \int_{x_1}^{x} k(x')\, dx' \right),
\tag{68}
$$

while the matching condition at the x_2 tells us that in the same allowed region we must have

$$
\Psi(x) = \frac{2C_2}{\sqrt{k(x)}} \times \sin\left(\frac{\pi}{4} + \int_{x}^{x_2} k(x')\, dx' \right).
\tag{69}
$$

14

To make these two solutions agree with each other, we need $C_1 = \pm C_2$ while

$$\sin\left(\frac{\pi}{4} + \int_{x_1}^{x} k(x')\, dx'\right) = \pm \sin\left(\frac{\pi}{4} + \int_{x}^{x_2} k(x')\, dx'\right) \quad \forall x. \tag{70}$$

In general

$$\sin\alpha = \pm \sin\beta \quad \text{if and only if} \quad \alpha \pm \beta = \pi \times \text{integer}, \tag{71}$$

so the sine condition (70) amounts to either

$$\frac{\pi}{2} + \int_{x_1}^{x} k(x')\, dx' + \int_{x}^{x_2} k(x')\, dx' = \pi \times \text{integer} \quad \forall x \tag{72}$$

or

$$\int_{x_1}^{x} k(x')\, dx' - \int_{x}^{x_2} k(x')\, dx' = \pi \times \text{integer} \quad \forall x. \tag{73}$$

Clearly, eq. (73) cannot be sustained for all x inside the allowed region, but eq. (72) is actually x independent since

$$\int_{x_1}^{x} k(x')\, dx' + \int_{x}^{x_2} k(x')\, dx' = \int_{x_1}^{x_2} k(x')\, dx', \tag{74}$$

so in order to have the same solution in the allowed region match physical solutions in both forbidden regions we need

$$\frac{\pi}{2} + \int_{x_1}^{x_2} k(x')\, dx' = \pi \times \text{integer}. \tag{75}$$

And since the integral here is positive, we need

$$\int_{x_1}^{x_2} k(x')\, dx' = \pi(n + \tfrac{1}{2}) \quad \text{for integer } n \geq 0, \quad i.\,e., \quad n = 0, 1, 2, 3, \ldots, \tag{76}$$

or equivalently

$$\int_{x_1}^{x_2} \sqrt{2m(E - V(x))}\, dx \;=\; \pi\hbar(n + \tfrac{1}{2}) \quad \text{for } n = 0, 1, 2, \ldots. \tag{77}$$

In terms of the classical particle motion, the LHS here — or rather twice the LHS — is the action integral over one complete period of the particle's motion,

$$S \;=\; \oint p(t)\, dx(t) \;=\; \int_{x_1}^{x_2} \left(p = +\sqrt{2m(E - V(x))}\right) dx \;+\; \int_{x_2}^{x_1} \left(p = -\sqrt{2m(E - V(x))}\right) dx$$

$$=\; 2 \times \int_{x_1}^{x_2} \sqrt{2m(E - V(x))}\, dx \tag{78}$$

sometimes called the *bounce action* for bouncing back and forth. In terms of this bounce action, eq. (77) becomes the (corrected) *Bohr–Sommerfeld quantization rule*

$$\oint p\, dx \;=\; 2\pi\hbar \times (n + \tfrac{1}{2}) \quad \text{for } n = 0, 1, 2, \ldots. \tag{79}$$

Historically, Niels Bohr and Arnold Sommerfeld came up with this ad hoc quantization rule in 1913 to explain the discrete energy levels of a harmonic oscillator or a hydrogen atom. This rule — originally written down as

$$\oint p\, dx \;=\; h \times \text{integer}, \tag{80}$$

— was a major part of the Old quantum theory, used until the modern quantum theory was developed in 1925.

For a harmonic oscillator, the Bohr–Sommerfeld quantization rule (79) happens to give exactly right energy levels. Indeed, for a classical harmonic oscillator

$$p^2 \;+\; \omega^2 m^2 x^2 \;=\; 2mE, \tag{81}$$

so in the (x, p) phase space the oscillations are ellipses with semi-axes $\sqrt{2mE}$ and $\sqrt{2mE}/m\omega$.

Consequently,

$$\oint p \, dx = \text{ellipse's area} = \pi \times \sqrt{2mE} \times \frac{\sqrt{2mE}}{m\omega} = \frac{2\pi mE}{m\omega} = \frac{2\pi E}{\omega}, \qquad (82)$$

so the Bohr–Sommerfeld quantization rule (79) tells us that

$$\frac{2\pi E}{\omega} = 2\pi\hbar(n + \tfrac{1}{2}) \quad \Longrightarrow \quad E = \hbar\omega(n + \tfrac{1}{2}). \qquad (83)$$

For most other quantum systems, the Bohr–Sommerfeld rule is in-exact. However, for most systems with an infinite (or at least very large) numbers of bound states, the Bohr–Sommerfeld rule becomes a good approximation for the energies E_n of the highly excited states $n \gg 1$, or at least for the energy differences $E_{n+1} - E_n$. Indeed, for the highly excited states the particle's motion becomes semiclassical, so we may use the WKB approximation for its wave function. And that's how we derived the Bohr–Sommerfeld equation (79) for the energy levels of the bound states.

Unbound Motion and Tunneling

Our next subject is the WKB approximation for the *un-bound* motion of a 1d particle over (or through) some potential barrier:

$$(84)$$
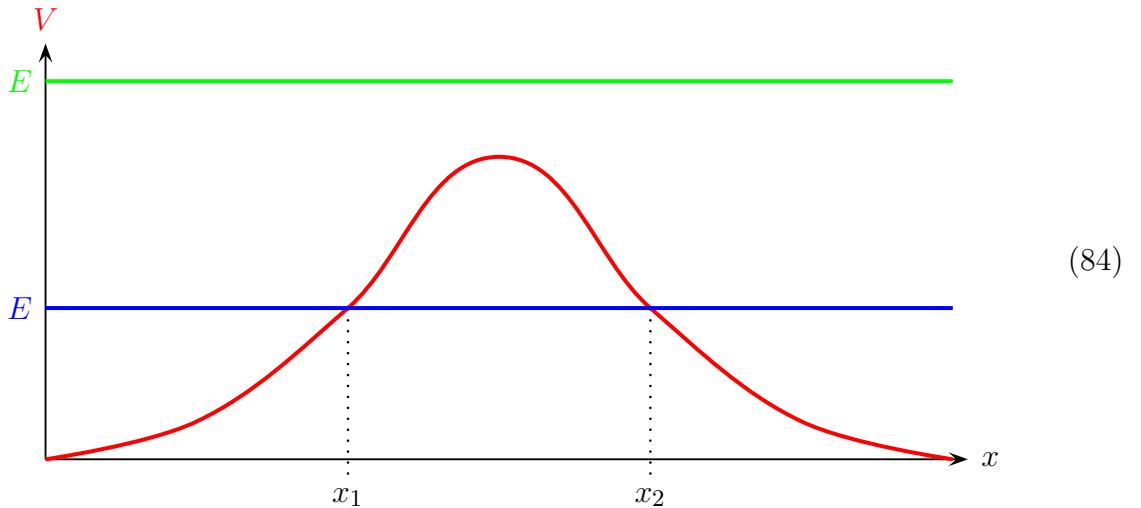
The green line here describes a particle with energy higher than the top of the barrier. Classically, such particle keeps flying in the same direction without stopping, and the WKB

approximation to the quantum particle gives the same result: forward motion — say, to the right, — without any left-moving component due to reflection,

$$\Psi_{\text{WKB}}(x) \;=\; \frac{\text{const}}{\sqrt{k(x)}} \times \exp\left(+i \int^{x} k(x')\,dx'\right) \;+\; \text{nothing else.} \tag{85}$$

Beyond the WKB approximation there is a bit of reflection, but as long as

$$\left|\frac{dk}{dx}\right| \;\ll\; k^2(x) \quad \forall\, x, \tag{86}$$

the WKB approximation is valid and the reflection is very weak. On the other hand, any abrupt discontinuity of the potential $V(x)$ — or a very rapid change for which $|k'| \gtrsim k^2$ — would break the WKB approximation and cause a substantial reflection, *cf.* discussion of the step potential in class and of the square barrier/well in homework set#6.

The blue line on the diagram (84) describes a particle with energy lower than the barrier's top. Classically, such a particle stops at the turning point x_1 and bounces back, so there is 100% reflection and no chance of getting through to the other side. In quantum mechanics, the particle is most likely reflected back, but it has a small chance of getting through the barrier; this is called *tunneling* under the barrier. To see how it works, we are going to use the WKB approximation for the wave function in the classically allowed regions $x < x_1$ and $x > x_2$, and in the classically forbidden region $x_1 < x < x_2$, and then use the Airy function matching across the boundary layers around the classical stopping points x_1 and x_2.

Let's start with the right allowed region $x > x_2$. Assuming initial particles come in from the left side, on the right side of the barrier the motion should be purely to the right, thus in the WKB approximation

$$\Psi_{\text{right}}(x) \;=\; \frac{e^{i\pi/4}\, A_2}{\sqrt{k(x)}} \times \exp\left(+i \int_{x_2}^{x} k(x')\,dx'\right)$$

$$\langle\!\langle \text{ where the } e^{i\pi/4} \text{ extra overall phase is for future convenience} \rangle\!\rangle$$

$$= \frac{A_2}{\sqrt{k(x)}} \times \cos\left(\frac{\pi}{4} + \int_{x_2}^{x} k(x')\,dx'\right) \;+\; i\frac{A_2}{\sqrt{k(x)}} \times \sin\left(\frac{\pi}{4} + \int_{x_2}^{x} k(x')\,dx'\right). \tag{87}$$

In the boundary layer around x_2, the first term on the bottom line becomes the irregular Airy

function Bi while the second term becomes the regular Airy function Ai. To the left of x_2, these Airy functions become respectively the growing and the shrinking WKB wave-functions for the forbidden region, specifically

$$\Psi_{\text{middle}}(x) \;=\; \frac{A_2}{\sqrt{\kappa(x)}} \times \exp\left(+\int_x^{x_2}\kappa(x')\,dx'\right) \;+\; \frac{i}{2} \times \frac{A_2}{\sqrt{\kappa(x)}} \times \exp\left(-\int_x^{x_2}\kappa(x')\,dx'\right). \quad (88)$$

Next, let's re-express the integrals of $\kappa(x')$ from x to x_2 in terms of similar integrals from x_1 to x,

$$\int_x^{x_2}\kappa(x')\,dx' \;=\; w \;-\; \int_{x_1}^{x}\kappa(x')\,dx', \quad (89)$$

$$\text{where } w \;=\; \int_{x_1}^{x_2}\kappa(x')\,dx', \quad \text{same } \forall x. \quad (90)$$

A point of notation: the little w is not the same as the big $W(x)$ I have used earlier in these notes; in particular, w is dimensionless while W has dimensionality of the classical action S or of the Planck constant $\hbar$.

Anyway, in light of eq. (89), we may rewrite the wave-function (88) for the forbidden region between x_1 and x_2 as

$$\begin{aligned}
\Psi_{\text{middle}}(x) \;=\;& \frac{A_2}{\sqrt{\kappa(x)}} \times \exp(+w) \times \exp\left(-\int_{x_1}^{x}\kappa(x')\,dx'\right) \\
&+ \frac{A_2}{\sqrt{\kappa(x)}} \times \frac{i}{2} \times \exp(-w) \times \exp\left(+\int_{x_1}^{x}\kappa(x')\,dx'\right).
\end{aligned} \quad (91)$$

Looking from the left turning point x_1, now its the first term in this formula which shrinks as we move into the forbidden region while the second term blows us, so in the boundary layer around the x_1 the first term turns into the regular Airy function Ai while the second term turns into the irregular Airy function Bi. In the allowed region to the left of the x_1,

both Airy functions become oscillating WKB solutions but with different phases, specifically

$$\Psi_{\text{left}}(x) = \frac{A_2}{\sqrt{k(x)}} \times \exp(+w) \times 2\sin\left(\frac{\pi}{4} + \int_x^{x_1} k(x')\,dx'\right)$$

$$+ \frac{A_2}{\sqrt{k(x)}} \times \frac{i}{2}\exp(-w) \times \cos\left(\frac{\pi}{4} + \int_x^{x_1} k(x')\,dx'\right). \tag{92}$$

Now let

$$\Phi(x) \overset{\text{def}}{=} \frac{\pi}{4} + \int_x^{x_1} k(x')\,dx' = \Phi_0 - \int^x k(x')\,dx', \tag{93}$$

for some integration constant Φ_0, then

$$\Psi_{\text{left}}(x) = \frac{A_2}{\sqrt{k(x)}} \times \exp(+w) \times 2\sin\Phi(x) + \frac{A_2}{\sqrt{k(x)}} \times \frac{i}{4}\exp(-w) \times 2\cos\Phi(x)$$

$$= \frac{A_2}{\sqrt{k(x)}} \times \exp(+w) \times \left(-i\exp(+i\Phi(x)) + i\exp(-i\Phi(x))\right)$$

$$+ \frac{A_2}{\sqrt{k(x)}} \times \frac{i}{4}\exp(-w) \times \left(\exp(+i\Phi(x)) + \exp(-i\Phi(x))\right) \tag{94}$$

$$= \frac{-iB_1}{\sqrt{k(x)}} \times \exp(+i\Phi(x)) + \frac{iA_1}{\sqrt{k(x)}} \times \exp(-i\Phi(x))$$

for

$$B_1 = A_2 \times \left(e^{+w} - \tfrac{1}{4}e^{-w}\right) \quad \text{and} \quad A_1 = A_2 \times \left(e^{+w} + \tfrac{1}{4}e^{-w}\right). \tag{95}$$

Finally, spelling out the $\Phi(x)$ on the bottom line of eq. (94) we get

$$\Psi_{\text{left}}(x) = \frac{-iB_1}{\sqrt{k(x)}} \times \exp\left(i\Phi_0 - i\int^x k(x')\,dx'\right) + \frac{+iA_1}{\sqrt{k(x)}} \times \exp\left(-i\Phi_0 + i\int^x k(x')\,dx'\right). \tag{96}$$

Thus, up to overall phases, A_1 is the amplitude of the right-moving wave while B_2 is amplitude of the left-moving wave, both on the left side of the barrier, while A_2 is the amplitude of the right-moving wave on the right side of the barrier. In other words, A_1 is the incident amplitude, B_1 is the reflected amplitude, and A_2 is the transmitted amplitude. Consequently,

the reflection probability is

$$R = \left|\frac{B_1}{A_1}\right|^2 = \left(\frac{e^{+w} - \frac{1}{4}e^{-w}}{e^{+w} + \frac{1}{4}e^{-w}}\right)^2 = \left(\frac{4 - e^{-2w}}{4 + e^{-2w}}\right)^2, \tag{97}$$
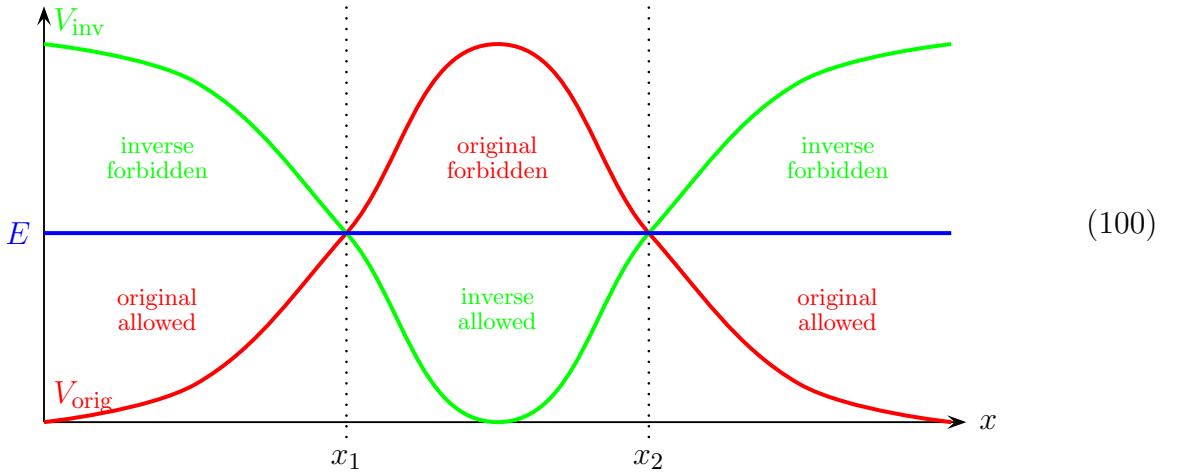
cf. eq. (95), while the transmission probability is

$$T = \left|\frac{A_2}{A_1}\right|^2 = \frac{1}{\left(e^{+w} + \frac{1}{4}e^{-w}\right)^2} = \frac{16e^{-2w}}{(4 + e^{-2w})^2}. \tag{98}$$

Physically, $2w$ is the *bounce action S* (in units of $\hbar$) *in the inverted potential*

$$V_{\mathrm{inv}}(x) = 2E - V(x) \implies (V - E)_{\mathrm{inv}} = -(V - E). \tag{99}$$

The inverse potential has the same turning points x_1 and x_2 as the original potential $V(x)$, but the classically allowed and the classically forbidden regions swap their places:

The barrier of the original potential becomes the well of the inverse potential, and inside this barrier/well region

$$k_{\mathrm{inv}}(x) = \kappa_{\mathrm{orig}}(x). \tag{101}$$

Consequently,

$$w = \int_{x_1}^{x_2} \kappa_{\mathrm{orig}}(x)\,dx = \int_{x_1}^{x_2} k_{\mathrm{inv}}(x)\,dx = \frac{1}{\hbar}\int_{x_1}^{x_2} p_{\mathrm{inv}}(x)\,dx = \frac{1}{2\hbar}\left[\oint_{1\,\mathrm{period}} p(t)\,dx(t)\right]_{V_{\mathrm{inv}}(x)}^{\mathrm{well\,of}}, \tag{102}$$

or in other words, $S_b = 2\hbar w$ is the bounce action of a particle bound in the well of the

21

inverse potential $V_{\text{inv}}(x)$. For classically thick and/or wide barriers, this bounce action is much larger than $\hbar$, hence

$$e^{-2w} \;=\; e^{-S_b/\hbar} \;\ll\; 1, \tag{103}$$

so we may approximate the transmission and the reflection coefficients for the barrier as

$$T \;=\; \frac{e^{-2w}}{(1+\frac{1}{4}e^{-2w})^2} \;\approx\; e^{-2w} \;=\; \exp(-S_b/\hbar) \;\ll\; 1, \tag{104}$$

while

$$R \;=\; 1 \;-\; T \;\approx\; 1 \;-\; \exp(-S_b/\hbar) \;\simeq\; 1. \tag{105}$$

Thus, a classically high and thick barrier is *almost* completely reflective, but there is a small probability of tunneling, namely

$$T \;\approx\; \exp(-S_b/\hbar) \;\ll\; 1. \tag{106}$$

To be precise, we have derived eqs. (98) and hence (106) for a smooth potential $V(x)$ which allows the WKB approximation inside the barrier and the Airy function matching across the barrier's ends x_1 and x_2. For the non-smooth potentials $V(x)$ — for example, for the square barrier of homework#6 (problem 2), — we generally have

$$T \;=\; C \times \exp(-S_b/\hbar) \;=\; C \times \exp(-2w) \tag{107}$$

where $S_b = 2\hbar w$ is the bounce action in the inverse potential, exactly as for a smooth $V(x)$, while C is an $O(1)$ pre-exponential factor depending on the discontinuities of the $V(x)$. For example, for the square barrier of the homework#6 we have

$$T \;=\; \frac{4E(V_b - E)}{4E(V_b - E) \;+\; V_b^2 \sinh^2(\kappa L)} \,, \tag{108}$$

cf. eq. (S.47) of the solutions to homework#6. For a square barrier $w = \kappa L$, so for $\kappa L \gg 1$

we may approximate

$$\sinh(\kappa L) \approx \tfrac{1}{2}\exp(\kappa L), \quad \sinh^2 \kappa L \approx \tfrac{1}{4}\exp(2\kappa L) = \tfrac{1}{4}\exp(2w), \tag{109}$$

and hence

$$T \approx \frac{4E(E - V_b)}{\tfrac{1}{4}V_b^2} \times \exp(-2w), \tag{110}$$

in perfect agreement with eq. (107) for

$$C = \frac{16E(V_b - E)}{V_b^2} = O(1). \tag{111}$$

Tunneling Examples

For a simple example of tunneling, consider the electrons pulled out from a metal cathode by the electric field $\mathcal{E}$. (Which we assume to be directed towards the cathode so the Coulomb force $F = -e\mathcal{E}$ pulls the electrons out.) The effective potential for an electron is constant inside the metal, rapidly rises at the metal edge, and then slowly decreases due to the electric field:

$$V(x) - E = V_0 - e\mathcal{E} \times x \tag{112}$$
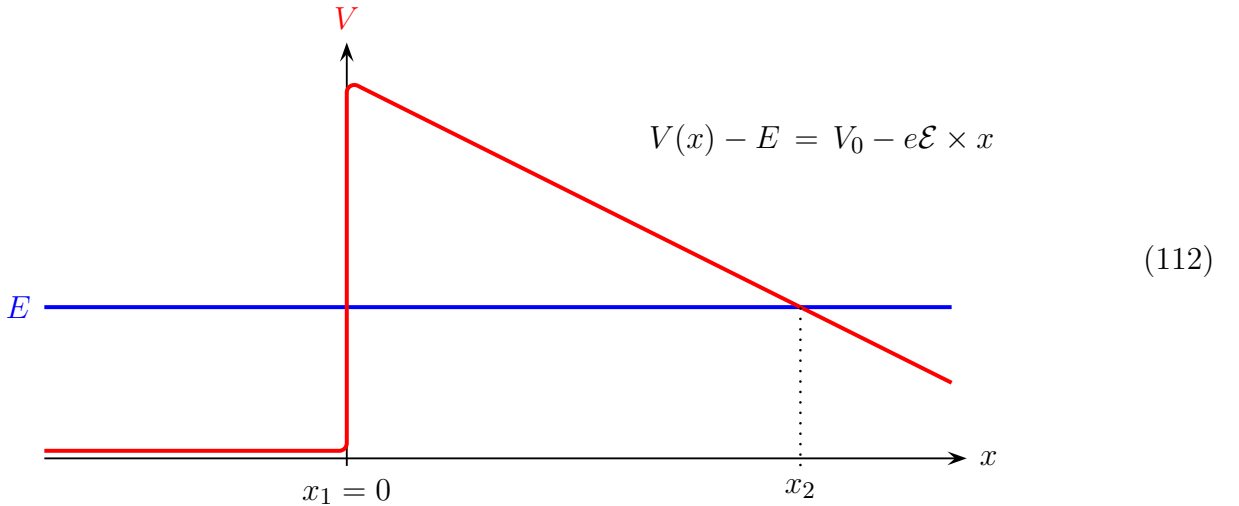
where V_0 is the metal's work function, *i.e.* the energy needed to pull an electron (of initial energy E at metal's Fermi level) out from the metal.

23

Classically, an electron does not have enough energy to simply fly out over the potential barrier, but in the quantum theory it can tunnel out. Specifically, the tunneling starts at the metal edge $x_1 = 0$ and ends at the point $x_2 = V_0/e\mathcal{E}$ where the potential drops below the electron's energy E. Between these points

$$\kappa(x) = \frac{\sqrt{2m(V(x) - E)}}{\hbar} = \frac{\sqrt{2m(V_0 - e\mathcal{E}x)}}{\hbar}, \tag{113}$$

hence

$$2w = 2\int_{x_1}^{x_2} \kappa(x)\, dx = 2\int_0^{V_0/e\mathcal{E}} \frac{\sqrt{2m(V_0 - e\mathcal{E}x)}}{\hbar}\, dx \tag{114}$$

$$= 2 \times \frac{\sqrt{2mV_0}}{\hbar} \times \frac{V_0}{e\mathcal{E}} \times \int_0^1 \sqrt{1 - \xi}\, d\xi \qquad \langle\!\langle \text{ where } x = (V_0/e\mathcal{E}) \times \xi \,\rangle\!\rangle$$

$$= \frac{2\sqrt{mV_0^3}}{\hbar e\mathcal{E}} \times \frac{2}{3} = \frac{\text{const}}{\mathcal{E}}. \tag{114}$$

Consequently, the probability of an electron hitting the cathode's edge to tunnel out through the potential barrier is

$$T = O(1) \times \exp\left(-\frac{\text{const}}{\mathcal{E}}\right), \tag{115}$$

and therefore the electric current from the cathode depends on the electric field as

$$I \propto \exp\left(-\frac{\text{const}}{\mathcal{E}}\right) \tag{116}$$

$$\star \qquad \star \qquad \star$$

For our second example, consider the centrifugal barrier keeping the radial motion of a particle away from the center. Back in homework set#4 we saw that

$$\hat{\mathbf{p}}^2 = \frac{\hat{\mathbf{L}}^2}{r^2} + \hat{p}_r^2 \tag{117}$$

where in the spherical coordinate basis

$$\hat{p}_r = -i\hbar\left(\frac{\partial}{\partial r} + \frac{1}{r}\right) = \frac{1}{r} \times \left(-i\hbar\frac{\partial}{\partial r}\right) \times r. \tag{118}$$

24

A wave-function of the form

$$\Psi(r, \theta, \phi) \;=\; \Psi_r(r) \times Y_{\ell,m}(\theta, \phi) \tag{119}$$

is an eigenstate of $\hat{\mathbf{L}}^2$ with the eigenvalue $\ell(\ell+1)\hbar^2$, so for a central potential $V(r)$ and energy E, the Schrödinger equation for this wave-function becomes

$$\frac{1}{r}\left(-\frac{\hbar^2}{2m}\frac{\partial^2}{\partial r^2} + \frac{\ell(\ell+1)\hbar^2}{2mr^2} + V(r) - E\right)\bigl(r\Psi_r(r)\bigr) \;=\; 0. \tag{120}$$

In other words, the radial wave-function $\Psi_r(r)$ — or rather $r \times \Psi_r(r)$ — obeys one-dimensional Schrödinger equation for an effective potential

$$V_{\text{eff}}(r) \;=\; V(r) \;+\; \frac{\mathbf{L}^2 = \ell(\ell+1)\hbar^2}{2mr^2}\,. \tag{121}$$

When the classical particle's path misses the center — which it always does unless $\mathbf{L} = 0$, — from the radial motion point of view it looks like it approaches the center, slows down due to the centrifugal potential, stops, turns around, and flies back away from the center. And its closest approach to the center is the turning point r_t in the effective potential (121). Quantum mechanically, the wave function extends beyond the classical turning point r_t, but it rapidly decreases as one moves into the classically forbidden region $r < r_t$. Let's use the WKB approximation to see how the radial function decreases with r for $r \to 0$.

Assume $\ell \neq 0$, then near the center

$$V_{\text{eff}}(r) \;-\; E \;=\; \frac{\ell(\ell+1)\hbar^2}{2mr^2} \;+\; \text{subleading terms for } r \to 0, \tag{122}$$

hence

$$\kappa^2(r) \;=\; \frac{2m}{\hbar^2} \times (V_{\text{eff}}(r) - E) \;\approx\; \frac{\ell(\ell+1)}{r^2} \quad \Longrightarrow \quad \kappa(r) \;\approx\; \frac{\sqrt{\ell(\ell+1)}}{r}\,. \tag{123}$$

The WKB approximation for a classically forbidden region is valid when

$$|\kappa'| \;\ll\; \kappa^2, \tag{124}$$

which for the $\kappa(r)$ at hand becomes

$$\frac{\sqrt{\ell(\ell+1)}}{r^2} \ll \frac{\ell(\ell+1)}{r^2} \iff \ell \gg 1. \tag{125}$$

Thus, the WKB approximation should be good for large angular momenta $\ell \gg 1$ but may break down for small ℓ like 1 or 2.

For large ℓ we may approximate

$$\sqrt{\ell(\ell+1)} \approx \ell + \tfrac{1}{2} \implies \kappa(r) \approx \frac{\ell+\tfrac{1}{2}}{r}. \tag{126}$$

Consequently,

$$\int_r^{r_t} \kappa(r')\, dr' \approx (\ell+\tfrac{1}{2}) \times \log\frac{r_t}{r} \tag{127}$$

and

$$\exp\left(\mp \int_r^{r_t} \kappa(r')\, dr'\right) \sim \exp\left(\mp(\ell+\tfrac{1}{2})\log\frac{r_t}{r}\right) = \left(\frac{r_t}{r}\right)^{\mp(\ell+\tfrac{1}{2})} \propto r^{\pm(\ell+\tfrac{1}{2})}. \tag{128}$$

For the WKB radial wave-functions in the near-center forbidden region this means

$$r \times \Psi_r(r) = A\sqrt{r} \times r^{+(\ell+\tfrac{1}{2})} + B\sqrt{r} \times r^{-(\ell+\tfrac{1}{2})}, \tag{129}$$

where the $\sqrt{r}$ factor on the RHS come from

$$\frac{1}{\sqrt{\kappa(r)}} = \frac{\sqrt{r}}{\sqrt{\ell+\tfrac{1}{2}}}, \tag{130}$$

while the LHS is $r \times \Psi_r(r)$ instead of $\Psi_r(r)$ because it's the $r \times \Psi_r(r)$ which appear in the radial Schrödinger equation (120). For the radial wave-function $\Psi_r(r)$ itself, eq. (129)

26

becomes

$$\Psi_r(r) \;=\; A \times r^{+\ell} \;+\; B \times r^{-\ell-1} \quad \text{when } r \to 0. \tag{131}$$

Moreover, the second term here blows up un-physically at the center leading to an infinite kinetic energy

$$\langle \Psi | \, \hat{H}_{\text{kinetic}} \, | \Psi \rangle \;=\; \frac{\hbar^2}{2m} \int d^3\mathbf{x}\, |\nabla\Psi|^2 \;\approx\; \int_0^{\cdots} dr\, r^2 \times \frac{B^2(\ell+1)^2}{r^{2\ell+4}} \;=\; +\infty, \tag{132}$$

so we must have $B = 0$ and therefore

$$\text{for } r \to 0: \quad \Psi_r(r) \;\propto\; r^{\ell}. \tag{133}$$

Note: we have derived eq. (133) using the WKB approximation, which is valid only for $\ell \gg 1$ but become inaccurate for small ℓ. Nevertheless, the asymptotic behavior (133) happens to be exact for all ℓ and even for $\ell = 0$. One may prove this result using differential equation techniques, but this goes beyond the scope of the present notes.

$$\star \qquad \star \qquad \star$$

For our last example of tunneling, consider nuclear fusion. Before two nuclei can fuse, they must approach each other within a distance of a few Fermi, but this cannot happens classically because of the Coulomb repulsion between the nuclei. At typical star-center temperatures — or even fusion bomb temperatures — the two initial nuclei do not have

enough energy to cross the Coulomb barrier

$$V(r) = \frac{Z_1 Z_2 e^2}{r} + V_{\text{nuclear}}(r) \tag{134}$$
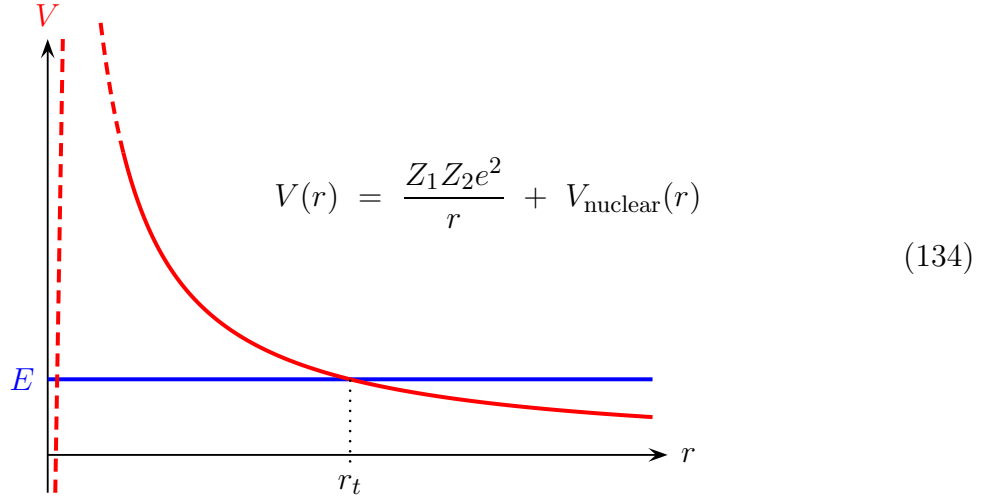
so they must tunnel towards each other under this barrier. The relative motion of the two nuclei is governed by the reduced one-body Hamiltonian

$$\hat{H}_{\text{red}} = \frac{\hat{\mathbf{P}}_{\text{red}}^2}{2m_{\text{red}}} + V(\hat{r}) \tag{135}$$

for the reduced mass

$$m_{\text{red}} = \frac{m_1 m_2}{m_1 + m_2}. \tag{136}$$

We are interested in the radial aspect of the relative motion described by the $\Psi_r(r)$, and just as we saw in the previous example it's governed by the effective potential

$$V_{\text{eff}} = \frac{Z_1 Z_2 e^2}{r} + V_{\text{nuclear}}(r) + \frac{\ell(\ell+1)\hbar^2}{2mr^2}. \tag{137}$$

For $\ell \neq 0$, the centrifugal term becomes very large and makes the wave function decrease as r^ℓ. In terms of tunneling probability T, this means

$$T[\ell \neq 0] \sim T[\ell = 0] \times \left(\frac{r_N}{r_c}\right)^{2\ell} \tag{138}$$

where r_N is the nuclear radius while r_c is the radius at which the centrifugal term in eq. (137) becomes larger than the two other terms. Numerically, $r_N \sim$ a few fm while $r_c \sim$ a few tens of fm, hence

$$T[\ell \neq 0] \ll T[\ell = 0], \tag{139}$$

so the fusion happens almost exclusively in the $\ell = 0$ partial wave AKA the s-wave.

Next, consider the nuclear potential V_{nuclear} and its effect on the tunneling. The nuclear potential is strong but very short-ranged: its magnitude starts with $V_N \sim$ a few MeV at $r \to 0$ but dies out for $r \gtrsim$ a few fm. In this range

$$\kappa = \frac{\sqrt{2m(V-E)}}{\hbar} \sim \frac{\text{a few}}{10 \text{ fm}}, \tag{140}$$

hence

$$\int\limits_{0}^{\text{few fm}} \kappa(x)\,dx \lesssim 1, \tag{141}$$

so the net effect of the nuclear potential term on the $w = \int \kappa\,dx$ is $O(1)$ or less. In other words, if we compare the bounce actions $S_b = 2\hbar w$ in the true inverse potential (including the V_{nuclear} term) versus purely Coulomb inverse potential, we get

$$\Delta w = w_{\text{true}} - w_{\text{Coulomb}} \lesssim 1, \tag{142}$$

hence net tunneling probability

$$T = C_{\text{true}} \times \exp(-2w_{\text{true}}) = C_{\text{true}} \times e^{-2\Delta w} \times \exp(-2w_{\text{Coulomb}}) = C' \times \exp(-2w_{\text{Coulomb}}) \tag{143}$$

for $C' = C_{\text{true}} \times e^{-2\Delta w} = O(1)$.

We are interested in the exponential factor in the tunneling probability (143), so let's calculate the tunneling rate for the purely Coulomb potential

$$V_{\text{eff}}(r) = V_{\text{Coulomb}}(r) + 0 = \frac{Z_1 Z_2 e^2}{r}. \tag{144}$$

The tunneling here is inward from the classical turning radius

$$r_t = \frac{Z_1 Z_2 e^2}{E} \quad \Longrightarrow \quad V(r) = E \tag{145}$$

all the way in to $r = 0$. In the classically forbidden region of $0 < r < r_t$, we have

$$
\begin{aligned}
\kappa(r) &= \frac{1}{\hbar}\sqrt{2m_{\text{red}}\left(\frac{Z_1 Z_1 e^2}{r} - E\right)} = \frac{1}{\hbar}\sqrt{2m_{\text{red}}\left(\frac{Z_1 Z_1 e^2}{r} - \frac{Z_1 Z_2 e^2}{r_t}\right)} \\
&= \frac{\sqrt{2m_{\text{red}}Z_1 Z_2 e^2}}{\hbar} \times \sqrt{\frac{1}{r} - \frac{1}{r_t}},
\end{aligned}
\tag{146}
$$

and consequently

$$2w = 2 \int_0^{r_t} \kappa(r)\, dr = 2\frac{\sqrt{2m_{\text{red}} Z_1 Z_2 e^2}}{\hbar} \times \int_0^{r_t} dr \sqrt{\frac{1}{r} - \frac{1}{r_t}}. \tag{147}$$

To evaluate the integral here, we change the integration variable:

$$r = r_t \times \sin^2\phi \quad \text{for} \quad 0 \le \phi \le \frac{\pi}{2}, \tag{148}$$

$$dr = 2r_t \sin\phi \cos\phi\, d\phi, \tag{149}$$

$$\frac{1}{r} - \frac{1}{r_t} = \frac{1}{r_t}\left(\frac{1}{\sin^2\phi} - 1\right) = \frac{1}{r_t \tan^2\phi}, \tag{150}$$

hence

$$dr \sqrt{\frac{1}{r} - \frac{1}{r_t}} = \frac{2r_t \sin\phi \cos\phi\, d\phi}{\sqrt{r_t}\tan\phi} = \sqrt{r_t} \times 2\cos^2\phi\, d\phi, \tag{151}$$

$$\int_0^{r_t} dr \sqrt{\frac{1}{r} - \frac{1}{r_t}} = \sqrt{r_t} \times \int_0^{\pi/2} 2\cos^2\phi\, d\phi = \sqrt{r_t} \times \frac{\pi}{2}, \tag{152}$$

and therefore

$$2w = 2\frac{\sqrt{2m_{\text{red}} Z_1 Z_2 e^2}}{\hbar} \times \frac{\pi}{2}\sqrt{r_t} = \pi\frac{\sqrt{2m_{\text{red}} Z_1 Z_2 e^2}}{\hbar} \times \sqrt{\frac{Z_1 Z_2 e^2}{E}} = \sqrt{\frac{E_0}{E}} \tag{153}$$

for

$$E_0 = 2m_{\text{red}} \times \left(\frac{\pi Z_1 Z_2 e^2}{\hbar}\right)^2, \tag{154}$$
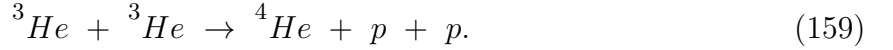
or numerically

$$E_0 = Z_1^2 Z_2^2 \frac{A_1 A_2}{A_1 + A_2} \times 0.98 \text{ MeV} \tag{155}$$

where $Z_{1,2}$ are the numbers of protons in each nucleus and $A_{1,2}$ are the net numbers of nucleons (protons+neutrons). Consequently, the tunneling probability — and hence the fusion rate of nuclei — depends on their reduced energy E as

$$\text{fusion rate}(E) = \mathcal{F} \times e^{-2w} = \mathcal{F} \times \exp\left(-\sqrt{\frac{E_0}{E}}\right) \tag{156}$$

where the pre-exponential factor $\mathcal{F}$ depends on the nuclear aspects of the fusion reaction rather than tunneling through the Coulomb barrier.

For example, consider the proton-proton fusion reaction — or rather a cycle of fusion reactions — which power most of the Sun's luminosity:

$$p + p \rightarrow D + e^+ + \nu, \tag{157}$$

$$D + p \rightarrow {}^3He + \gamma, \tag{158}$$

$${}^3He + {}^3He \rightarrow {}^4He + p + p. \tag{159}$$

There are some alternative reaction chains to the direct fusion (159) of two helium-3 nuclei, but they are not germane to the present discussion. In any case, the rate of the proton-proton fusion cycle is limited by the first reaction (157): Unlike the other fusion reactions, it involves weak interactions to turn one of the protons into a neutron in the deuterium nucleus D, so it has a much smaller pre-exponential factor $\mathcal{F}$ than the other fusion reactions.

Besides a small pre-exponential factor, the reaction (157) also has a very small exponential factor for the average proton pair in the Sun. Indeed, the central region of the sun has temperature $T \approx 15.5 \cdot 10^6$ K, so the average proton pair in that region has reduced thermal energy $\langle E \rangle = \frac{3}{2} k_B T \approx 2.0$ keV while $E_0 = 0.49$ MeV, thus

$$\exp\left(-\sqrt{\frac{E_0}{\langle E \rangle}}\right) \sim 10^{-7}. \tag{160}$$

Because of this very small tunneling factor, the thermally-averaged proton pairs rarely fuse. Instead, most fusion happens for the higher-energy protons at the tail end of the Boltzmann energy distribution

$$N(E) \propto \exp(-E/k_B T), \tag{161}$$

so the net fusion rate is proportional to

$$\langle \text{net rate} \rangle \propto \int_0^\infty dE \, N(E) \times \text{rate}(E) \propto \int_0^\infty dE \, \exp\left(-\frac{E}{k_B T} - \sqrt{\frac{E_0}{E}}\right). \tag{162}$$

To estimate this integral, let's change the integration variable from E to

$$\nu = \frac{E}{E_0^{1/3}(k_b T)^{2/3}}, \tag{163}$$

thus

$$\frac{E}{k_b T} + \sqrt{\frac{E_0}{E}} = \sqrt[3]{\frac{E_0}{k_B T}} \times f(\nu) \quad \text{for} \quad f(\nu) = \nu^{-1/2} + \nu \tag{164}$$

and therefore

$$\langle \text{net rate} \rangle \propto \int_0^\infty d\nu \, \exp\left(-\sqrt[3]{\frac{E_0}{k_B T}} \times f(\nu)\right). \tag{165}$$

For $k_B T \ll E_0$, the integrand here becomes sharply peaked at the minimum of $f(\nu)$, hence

$$\langle \text{net fusion rate} \rangle = (\text{pre-exponential factor } \mathcal{A}) \times \exp\left(-\sqrt[3]{\frac{E_0}{k_B T}} \times \min[f(\nu)]\right). \tag{166}$$

Specifically,

$$\frac{df(\nu)}{d\nu} = \frac{-1}{2\nu^{3/2}} + 1 \quad \text{which vanishes for} \quad \nu = 2^{-2/3}, \tag{167}$$

hence

$$\min[f(\nu)] = f(\nu = 2^{-2/3}) = 2^{+1/3} + 2^{-2/3} = \frac{3}{2^{2/3}}, \tag{168}$$

and therefore

$$\langle \text{net fusion rate} \rangle = \mathcal{A} \times \exp\left(-\sqrt[3]{\frac{E_0}{k_B T}} \times \frac{3}{2^{2/3}}\right) = \mathcal{A} \times \exp\left(-\sqrt[3]{\frac{T_0}{T}}\right) \tag{169}$$

for

$$T_0 = \frac{27 E_0}{4 k_B} \approx 76.7 \cdot 10^9 \text{ K} \times Z_1^2 Z_2^2 \frac{A_1 A_2}{A_1 + A_2}. \tag{170}$$

In particular, for the proton-proton fusion reaction (157) we have $T_0 = 38.6 \cdot 10^9$ K while the temperature of the Sun's center is only $T = 15.5 \cdot 10^6$ K, thus

$$\exp\left(-\sqrt[3]{\frac{T_0}{T}}\right) \sim 10^{-6}. \tag{171}$$

On top of this small factor, the pre-exponential factor $\mathcal{A}$ is also very small due to the weak

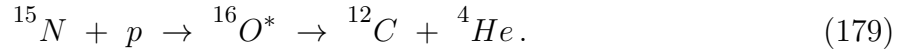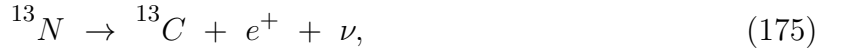interactions involved in the proton-proton fusion,

$$\mathcal{A}_{pp} \sim 10^{-4} \text{ yr}^{-1}, \tag{172}$$

thus

$$\frac{\text{net fusion rate}}{\text{per proton}} \sim 10^{-10} \text{ yr}^{-1}, \tag{173}$$

and that's how the Sun is expected to keep shining for 10^{10} years.

Now consider the CNO fusion cycle which powers the stars heavier than the Sun:

$$^{12}C + p \rightarrow {}^{13}N + \gamma, \tag{174}$$

$$^{13}N \rightarrow {}^{13}C + e^+ + \nu, \tag{175}$$

$$^{13}C + p \rightarrow {}^{14}N + \gamma, \tag{176}$$

$$^{14}N + p \rightarrow {}^{15}O + \gamma, \tag{177}$$

$$^{15}O \rightarrow {}^{15}N + e^+ + \nu, \tag{178}$$

$$^{15}N + p \rightarrow {}^{16}O^* \rightarrow {}^{12}C + {}^4He. \tag{179}$$

For this cycle, the rate-limiting reaction is the nitrogen-proton fusion (177), for which

$$E_0 = 45.1 \text{ MeV} \quad \text{and} \quad T_0 = 3.53 \cdot 10^{12} \text{ K}, \tag{180}$$

so at the center-of-the Sun conditions the CNO cycle is suppressed by a much smaller exponential factor

$$\exp\left(-\sqrt[3]{\frac{T_0}{T}}\right) \sim 10^{-26.5} \tag{181}$$

than the proton-proton cycle. On the other hand, in the CNO cycle the weak interaction work through beta-decays after the fusion has already happened rather than during the fusion itself, so its pre-exponential factor

$$\mathcal{A}_{\text{CNO}} \sim 10^{+14.5} \text{ yr}^{-1} \tag{182}$$

is much larger than for the proton-proton cycle. Altogether, in the Sun

$$\frac{\text{power produced by the CNO cycle}}{\text{power produced by the proton-proton cycle}} \sim \frac{1}{60}, \tag{183}$$

In other stars, this pp to CNO ratio raises very rapidly with the central temperature of

the star, which in turn increases with the star's mass. Thus, a main-sequence star of mass $M = 1.3\ M_\odot$ has $T_c \approx 18 \cdot 10^6$ K, at which temperature the pp cycle and the CNO cycle provide similar fusion powers. And in still heavier main-sequence stars — which have even higher central temperatures — it's the CNO cycle which privides most of the fusion power.

WKB in 3 Dimensions

In $d > 1$ dimensions, the WKB approximation is a lot less powerful than in 1 dimension: it does not give us the whole wave-function, although it helps to find its phase. This is particularly useful when dealing with interference between 2 or more semi-classical trajectories leading to the same places; for example, a 2-slit experiment with an electron beam.

To see how this works, let's start with the WKB ansatz,

$$\Psi(\mathbf{x}, t) \;=\; \sqrt{\rho(\mathbf{x}, t)} \times \exp\left(\frac{i}{\hbar} W(\mathbf{x}, t)\right), \tag{184}$$

plug this wave-function into the Schrödinger equation, and then neglect terms of relative order $O(\hbar^2)$. Proceeding exactly as we did in eqs. (4) through (20) for $d = 1$, we end up with

$$\dot{W} \;+\; \frac{1}{2m}\left(\nabla W\right)^2 \;+\; V \;=\; 0, \tag{185}$$

$$\dot{\rho} \;+\; \frac{1}{m}\nabla \cdot (\rho \nabla W) \;=\; 0, \tag{186}$$

for a time-dependent state, or for a stationary state of energy E,

$$\left(\nabla W(\mathbf{x})\right)^2 \;=\; 2m(E - V(x)), \tag{187}$$

$$\nabla \cdot (\rho \nabla W) \;=\; 0. \tag{188}$$

Similar to the 1d case, eq. (185) is the Hamilton–Jacobi equation for the classical principal function $W(\mathbf{x}, t)$, so we may identify $\nabla W(\mathbf{x}, t)$ with the classical momentum $\mathbf{p}(\mathbf{x}, t)$ of a particle which arrives to the point $\mathbf{x}$ at time t starting with some fixed place $\mathbf{x}_0$ at some

fixed time t_0. Alas, eq. (187) gives us the magnitude of this classical momentum,

$$|\mathbf{p}(\mathbf{x})| = \sqrt{2m(E - V(\mathbf{x}))}, \tag{189}$$

but not its direction. Or in terms of the $W(x)$, eq. (187) gives us the magnitude but not the direction of the gradient $\nabla W(\mathbf{x})$, and that's not enough information to find the $W(\mathbf{x})$ itself. Likewise, eq. (188) does not give us enough information to find the $\rho(\mathbf{x})$.

However, eq. (185) for the phase of the wave-function $\Psi(\mathbf{x}, t)$ is not completely useless. For a semi-classical motion, when we know the classical path $\mathbf{x}(t)$ from $\mathbf{x}(t_1) = \mathbf{x}_1$ to $\mathbf{x}(t_2) = \mathbf{x}_2$, the phase $W(\mathbf{x}_2, t_2)$ obtains as a classical principal function

$$W(\mathbf{x}_2, t_2) = \int_{t_1}^{t_2} L(\mathbf{x}(t), \dot{\mathbf{x}}(t)) \, dt \quad \text{along the classical path,} \tag{190}$$

hence

$$\text{phase}(\Psi(\mathbf{x}_2, t_2)) - \text{phase}(\Psi(\mathbf{x}_1, t_1)) = \frac{1}{\hbar} \int_{t_1}^{t_2} L(\mathbf{x}(t), \dot{\mathbf{x}}(t)) \, dt \quad \text{along the classical path.} \tag{191}$$

For a motion of given energy E,

$$L(\mathbf{x}, \dot{\mathbf{x}}) \, dt = \mathbf{p} \cdot d\mathbf{x} - H(\mathbf{x}, \mathbf{p}) \, dt = \mathbf{p} \cdot d\mathbf{x} - E \, dt, \tag{192}$$

hence

$$W(\mathbf{x}_2, t_2) = \int_{\substack{\text{classical path} \\ \text{from } \mathbf{x}_1 \text{ to } \mathbf{x}_2}} \mathbf{p}(t) \cdot d\mathbf{x}(t) - E \times (t_2 - t_1), \tag{193}$$

so for a stationary-state limit

$$\Psi(\mathbf{x}, t) = \Psi(\mathbf{x}) \times e^{-iEt/\hbar} \tag{194}$$

of semiclassical motion, we have

$$\text{phase}(\Psi(\mathbf{x}_2)) - \text{phase}(\Psi(\mathbf{x}_1)) = \frac{1}{\hbar} \int_{\mathbf{x}_1}^{\mathbf{x}_2} \mathbf{p}(t) \cdot d\mathbf{x}(t) \quad \text{along the classical path.} \tag{195}$$

Now consider an interference experiment like a 2-slit experiment for the electrons. If

there are two different semi-classical ways for a particle to get from the same point A to the same point B, then

$$\Psi_{\text{net}}(\mathbf{x}_B) \;=\; \Psi_1(\mathbf{x}_B) \;+\; \Psi_2(\mathbf{x}_B) \tag{196}$$

and hence

$$
\begin{aligned}
|\Psi_{\text{net}}|^2 \;&=\; \rho_1 \;+\; \rho_2 \;+\; 2\sqrt{\rho_1\rho_2}\times\cos(\Delta\phi) \\
\text{for}\quad \Delta\phi \;&=\; \text{phase}(\Psi_1(\mathbf{x}_B)) \;-\; \text{phase}(\Psi_2(\mathbf{x}_B)).
\end{aligned}
\tag{197}
$$

The WKB approximation in 3D does not give us the magnitudes $\rho_1 = |\Psi_1|^2$ and $\rho_2 = |\Psi_2|^2$ of the wave functions obtaining via each path, but it does gives us the phase difference $\Delta\phi$. Indeed, evaluating eq. (195) for each classical path, we get

$$\Delta\phi \;=\; \frac{1}{\hbar}\left[\int\limits_{\text{path\#1}}\mathbf{p}\cdot d\mathbf{x} \;-\; \int\limits_{\text{path\#2}}\mathbf{p}\cdot d\mathbf{x}\right]. \tag{198}$$

Gravitationally Induced Neutron Interference

As an example of WKB-bases eq. (198) for a 2-path interference, consider the 1975 experiment by Colella, Overhauser, and Werner which demonstrated *gravitationally induced neutron interference*. Schematically, their experiment looked like this:

(199)
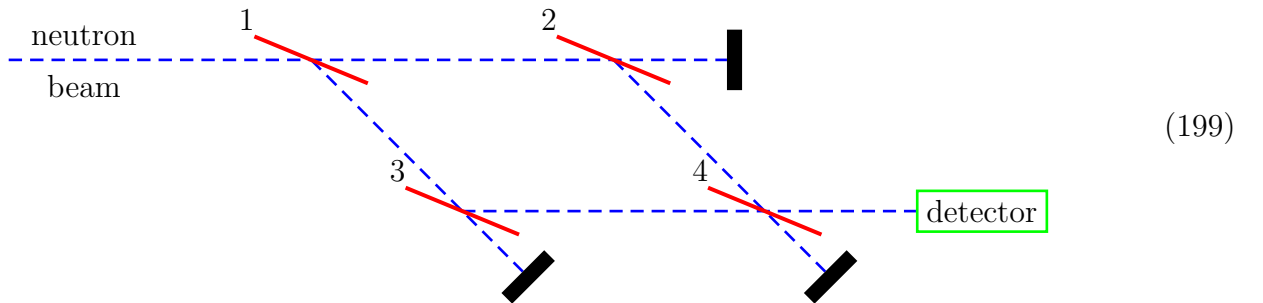
where the red lines indicate semi-transparent neutron mirrors. A neutron can reach the detector along either of the two paths 124 and 134, hence interference with relative phase

$$\Delta\phi \;=\; \frac{1}{\hbar}\left[\int\limits_{124}\mathbf{p}\cdot d\mathbf{x} \;-\; \int\limits_{134}\mathbf{p}\cdot d\mathbf{x}\right]. \tag{200}$$

Together, the two paths form a parallelogram of size a (segments 12 and 34) by b (segments 13 and 24), and the whole experiment — the mirrors and the detector — is mounted

on a tilting platform. As the platform tilts, the segments 12 and 34 remain horizontal but have their elevations different by

$$\Delta z \;=\; b \sin \alpha \times \sin \theta_{\text{tilt}} \,. \tag{201}$$

On the other hand, the segments 13 and 24 are tilted but they are parallel to each other and the separation between them is purely horizontal. Consequently, when we consider the classical actions of a neutron flying along each path, the segments 13 and 24 yield equal contributions to the two path's actions,

$$\int_{13} \mathbf{p} \cdot d\mathbf{x} \;=\; \int_{24} \mathbf{p} \cdot d\mathbf{x}, \tag{202}$$

regardless of the platform tilt. Therefore,

$$\int_{124} \mathbf{p} \cdot d\mathbf{x} \;-\; \int_{134} \mathbf{p} \cdot d\mathbf{x} \;=\; \int_{12} \mathbf{p} \cdot d\mathbf{x} \;-\; \int_{34} \mathbf{p} \cdot d\mathbf{x} \;=\; a \times p_{\text{cl}}(12) \;-\; a \times p_{\text{cl}}(34), \tag{203}$$

where the second equality stems from the classical momentum staying constant along a horizontal segment. However, $p_{\text{cl}}(12) \neq p_{\text{cl}}(34)$ because the two horizontal segments have slightly different gravitational potentials,

$$\Delta V \;=\; m_n g \Delta z \tag{204}$$

and hence slightly different kinetic energies of neutrons flying along these segments. This difference is very small compared to the kinetic energies themselves, hence

$$p_{\text{cl}}(12) \;-\; p_{\text{cl}}(34) \;\approx\; \frac{\Delta V}{v} \tag{205}$$

where $v = p/m$ is the classical neutron's velocity. Altogether, for the Colella, Overhauser, and Werner setup,

$$\begin{aligned}
\Delta \phi \;&=\; \frac{a}{\hbar} \left(p_{\text{cl}}(12) - p_{\text{cl}}(34) \right) \;=\; \frac{a}{\hbar} \times \frac{\Delta V}{v} \;=\; \frac{a}{\hbar} \times \frac{m_n g \Delta z}{v} \\
&=\; \frac{m_n g}{\hbar v} \times a \times \Delta z \;=\; \frac{m_n g}{\hbar v} \times a \times b \sin \alpha \times \sin \theta_{\text{tilt}} \\
&=\; \frac{m_n g}{\hbar v} \times \text{Area} \times \sin \theta_{\text{tilt}} \,.
\end{aligned} \tag{206}$$

To keep the interference pattern clear, Colella *et al* needed a beam of neutrons with the same velocity v. They started with a beam of thermal neutrons from a nuclear reactor

— which had a Maxwell distribution of velocities peaking between 2 and 3 km/s, — and then used Bragg scattering off a crystal to produce a secondary beam of neutrons having a specific De Broglie wavelength $\lambda = 1.445$ Å. This secondary beam had neutrons with uniform velocities

$$v \;=\; \frac{1}{m_n} \times \frac{2\pi\hbar}{\lambda} \;=\; 2737 \text{ m/s}, \tag{207}$$
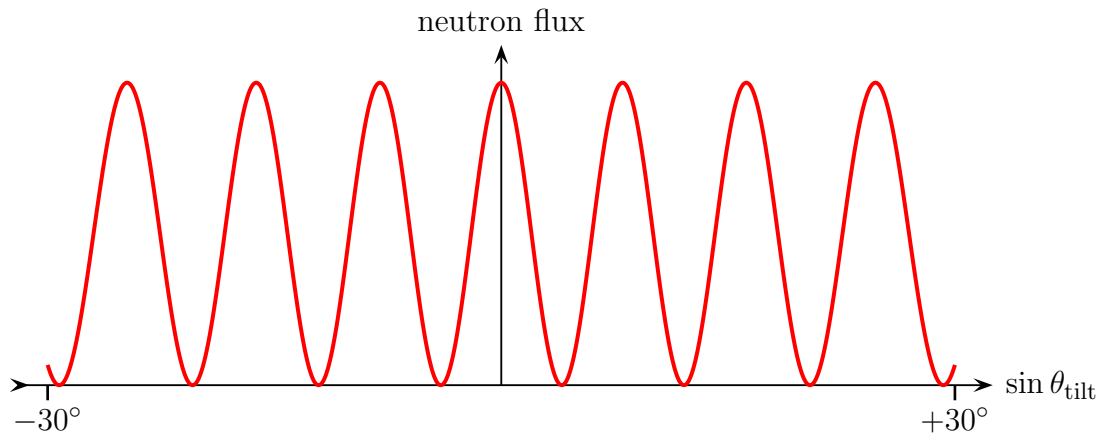
hence

$$\frac{m_n g}{\hbar v} \;=\; \frac{m_n^2 g\lambda}{2\pi\hbar^2} \;=\; 9.05 \text{ cm}^{-2}. \tag{208}$$

The interference region in the Colella *et al* experiment had area $ab\sin\alpha \approx 5 \text{ cm}^2$, thus

$$\frac{\Delta\Phi}{2\pi} \;\approx\; 7.2 \times \sin\theta_{\text{tilt}}, \tag{209}$$

so by slowly varying the tilt angle θ_{tilt} between $-30°$ and $+30°$ they saw 7 peaks and 8 troughs of the interference pattern. Here is the *idealized* plot:

And were they able to tilt all the way from $-90°$ to $+90°$, they would have gotten

38